This is a preprint, the final version is subject to change, of the American Mineralogist (MSA)
Cite as Authors (Year) Title. American Mineralogist, in press.
(DOI will not work until issue is live.) DOI: http://dx.doi.org/10.2138/am-2014-4654

Revision 1

Etch-pit size, dissolution rate, and time in the experimental dissolution of olivine: Implications for estimating olivine lifetime at the surface of Mars

Michael A. Velbel[1,2]

[1]Department of Geological Sciences, 206 Natural Science Building, 288 Farm Lane, Michigan State University, East Lansing, MI 48824-1115

[2]Division of Meteorites, Department of Mineral Sciences, National Museum of Natural History, Smithsonian Institution, 10th and Constitution Avenues NW, Washington, DC 20560-0119

Abstract

A variety of approaches have been used to estimate when and how long liquid water was present at the surface of Mars. The olivine dissolution-lifetime application suggested by Stopar et al. (2006) and Olsen and Rimstidt (2007) is here adapted and tested at the scale of individual etch-pits using published data from an experimental system in which the volume of mineral removed and the duration of the mineral-removal episode are known. Different assumptions about the specific geometry of etch-pits on olivine result in surface-area estimates that vary by less than a factor of two from the simple hemispherical pit used in the calculations. Given that other sources of uncertainty in mass-time relationships of silicate-mineral dissolution during natural weathering can be up to four orders-of-magnitude, the effects of differing geometric assumptions about the shapes and surface areas of the etch-pits are negligible.

Using compiled experimentally determined forsterite dissolution rates and the imaged etch-pit sizes from experiments recovers the duration of the experiment that produced the imaged etch-pits to within less than a factor of two. This suggests that extensively etched olivine surfaces imply a dominance of the etch-pit walls over the bulk surface between the etch-pits during olivine corrosion. The approach adopted here recovers the timescales of experimental etch-pit production on olivine at STP and extreme undersaturation of the solution with respect to olivine in experiments where pH is known. Continued progress in understanding the fundamentals of olivine dissolution kinetics will narrow the ranges of uncertainty in mineral-lifetime estimates at Mars' surface in support of constraining the compositions and duration of potentially habitable aqueous solutions on Mars.

Keywords: Olivine, geochemical kinetics, dissolution, etch-pits, Mars

Introduction

Dissolution of rock-forming minerals is a major source of solutes to terrestrial natural waters (e.g., Berner and Berner 2012) and likely contributes similarly to such aqueous solutions as may have existed on Mars (e.g., Velbel 2012). Consequently, the rates, processes, and mechanisms of mineral dissolution are of broad significance to many disciplines within the Earth sciences, and are well-studied (Brantley et al. 2008). Olivine, $(Mg,Fe)_2SiO_4$, is one of the major rock-forming minerals on Earth (Deer et al. 1992) and throughout the Solar System (Hutchison 2004). In Earth's surface environment, olivine weathers more rapidly than any other common naturally occurring orthosilicate (Velbel 1999) or other major rock-forming silicate mineral (Goldich 1938; Wilson 2004). Consequently, olivine does not usually persist in most soils (even soils developed on olivine-bearing parent materials), sediments, or sedimentary rocks (Delvigne et al. 1979; Morton and Hallsworth 1999; Wilson 2004). Recent research (Velbel 2009) has brought understanding of dissolution features and their implications for reaction processes on naturally weathered olivine grains closer to the higher level of understanding of similar phenomena on other, more widespread and therefore better-studied rock-forming minerals in Earth surface environments.

Etch-pits, which are crystallographically distributed and oriented dissolution mineral-surface features of negative relief (e.g., Wilson 1975; Berner 1978) are widely recognized textural indicators of site-selective mineral-surface destruction during corrosive dissolution (etching). Experimental etching of olivine by strong acids, bases, and complexing agents has long been used to study defects, dislocations, rock and mineral deformation, and cosmic-ray exposure tracks in naturally occurring olivines and their synthetic counterparts (Young 1969; Grossman et al. 1971; Wegner and Christie 1974, 1976; Kirby and Wegner 1978; Inoue et al. 1981; Tang and Dieckmann 2011, 2012). A variety of etch-pit (etch figure) morphologies have been experimentally produced on euhedral or cleaved single crystals or artificially polished surfaces of known low-index crystallographic orientation - usually (100) or (010), less commonly (001). Etch-pit shapes include rectangular pyramidal and square-based pyramidal pits on (010) and (100) that are elongate in the [001] and [010] directions, respectively (Wegner and Christie 1974, 1976; Kirby and Wegner 1978); oval- and diamond-shaped etch-pits on (001) surfaces elongate in the [010] direction and shorter in the [100] direction, and arrays of diamond-shaped pits aligned either in the [100] direction or in some other orientation in the *x*-*y* plane (Wegner and Christie 1974, 1976; Kirby and Wegner 1978; Inoue et al. 1981). The elongation of diamond shaped etch-pits and their alignment with etch channels in naturally altered (weathered or serpentinized) olivine imaged in TEM (Eggleton 1986; Banfield et al. 1990; Boudier et al. 2010), and the orientations of conical etch-pits inferred from the SEM morphological observations of etch-pits (Fig. 1) on naturally weathered olivine (Velbel 2009), are all consistent with the observations from etching experiments.

Etch-pits are evidence for olivine reactivity in a variety of natural and experimental settings relevant to environmental and materials applications such as natural weathering, carbon dioxide sequestration by olivine-rich rocks, and synthesis of porous or nanostructured materials from natural olivine (Giammar et al. 2005; Bearat et al. 2006;

Velbel 2009; Haug et al. 2010; King et al. 2010, 2011; Daval et al. 2011; Lafay et al. 2012). In both natural and artificial reactions, insight can be retrieved from relationships between the volume of mineral removed during dissolution, the rate of removal, and the duration of the dissolution episode. For example, mineral-lifetime estimates relating olivine grain size and dissolution rate (both known) and time (unknown) are combined with the widespread persistence of olivine at the surface of Mars determined from orbital and surface missions to place limits on the maximum duration of aqueous alteration of Mars' surface materials (Stopar et al. 2006; Olsen and Rimstidt 2007). Similar approaches can be applied to smaller-scale olivine dissolution as well. Wedges or wedge-shaped notches along fractures or dislocation arrays are the observed two-dimensional expression of olivine etch-pits in cross-section (e.g., in polished thin-sections), from which the occurrence of three-dimensional etch-pits is inferred based on the etch-pit shape model and the geometric relationships between etch-pits and the surfaces they intersect (Velbel 2009). Such wedge-shaped notches have been imaged in reports from naturally weathered olivine (Velbel 2009), experimentally altered olivine (King et al. 2011), and olivine in Mars meteorites including meteorite finds recovered after long terrestrial exposure and the Mars meteorite Nakhla, recovered promptly after witnessed fall in 1911 (Velbel 2012; Lee et al. 2013). In Mars meteorite falls, aqueous alteration is almost entirely of Martian origin, whereas in finds any specific aqueous alteration feature may be either pre-terrestrial or terrestrial (Velbel, 2012). Etch-pits are too small to be imaged by the instruments deployed by Mars surface missions, but they have been imaged in Mars meteorites, allowing the extension of the whole-grain-scale approach of Stopar et al. (2006) and Olsen and Rimstidt (2007) to smaller spatial scales.

Dissolution at a mineral's surface may occur from both bulk surfaces and specific mineral-surface sites such as strained crystal volumes around dislocations (e.g., Berner 1978; Brantley et al. 1986; Lüttge et al. 1999; Lasaga and Lüttge 2001). The relative proportions of site-specific dissolution and dissolution at bulk-surfaces varies among different minerals and with different extent of dissolution of the same mineral (Velbel et al. 2007). This paper tests the hypothesis that dissolution of olivine in ambient temperature (Earth surface) aqueous solutions occurs predominantly at the walls of etch-pits, and that additional retreat of bulk surface between etch-pits is not required to explain quantitative relationships among etch-pit size, olivine dissolution rate, and the duration of the dissolution episode. The hypothesis is formulated as geometric assumptions from which timescales for formation of etch-pits on olivine experimentally corroded during dissolution-kinetics experiments are here estimated from the measured maximum etch-pit size and compilations of dissolution rates from the extensive body of literature on the experimental geochemical dissolution kinetics of olivine in water at ambient temperatures. This study uses an approach (Velbel et al. 2007) that is similar to but smaller in scale than published approaches to mineral-lifetime estimates (Stopar et al. 2006; Olson and Rimstidt 2007). Using this approach, (1) the hypothesis is tested against experimental data, and (2) the dissolution-lifetime application suggested by Stopar et al. (2006) and Olsen and Rimstidt (2007) is tested for the first time in a system where mineral dissolution rate, volume of mineral removed, and the duration of the mineral-removal episode are all known.

This is a preprint, the final version is subject to change, of the American Mineralogist (MSA)
Cite as Authors (Year) Title. American Mineralogist, in press.
(DOI will not work until issue is live.) DOI: http://dx.doi.org/10.2138/am-2014-4654 6/4

METHOD

The hypothesis stated above is formulated as an equation relating the volume of material removed from an etch-pit of a given dimension, the corresponding surface area, and the known published experimentally determined olivine dissolution rate to time, the duration of the experiment in which the observed etch-pit was formed. This section presents the assumptions invoked in the equations, including the justification for a simplified description of the etch-pit geometry.

Previous research monitoring mineral-surface retreat during dissolution using vertical scanning interferometry (Lüttge et al. 1999; Lasaga and Lüttge 2001) observed that bulk experimental dissolution of several plagioclase feldspars involves dissolution from both etch-pits and retreat (lowering) of the surface between them. However, Velbel et al. (2007) have shown that the dissolution process may operate differently on different silicate minerals; further consideration of their geometric reasoning allows extension of their inferences to different occurrences of the same mineral, at different stages of surface modification by site-selective etching.

Previous work on garnet (Velbel et al. 2007) and olivine (Velbel 2009) suggests that, at all but the earliest stages of silicate-mineral dissolution during natural weathering, large fractions (in some cases, the entirety) of exposed grain surface consists of walls of coalesced etch-pits, with little or no surface other than etch-pit walls. Similarly, cross-sections of grain perimeters, internal fractures, and the walls of "etch channels" can consist entirely of overlapping etch-pit walls, even if etching has affected only the near-surface portion of the olivine (Velbel 2009). Internal surface formed by corrosion consists by definition entirely of etch-pit walls. Consequently, from local etch-pit saturation of surface onward, the entire mineral surface consists of etch-pit walls, and there is no other surface (Fig. 1, outlined area; other examples are shown by Velbel 2009). At earlier stages of olivine dissolution, there is unetched surface between the etch-pits (as in Fig. 1, arrows). However, the fact that such unetched surface does not survive at more advanced stages of olivine dissolution (Fig. 1, outlined area) suggests that etch-pit edges are consumed faster by lateral growth of etch-pits (dissolution of etch-pit walls and edges) than by bulk-surface lowering, unlike feldspar dissolution. In this way, natural weathering of olivine (Velbel 2009) is similar to natural dissolution of garnet (Velbel et al. 2007). Given the greater extent of weathering to which naturally weathered silicate-mineral grains have been subjected compared with short-duration ambient-temperature experimental dissolution of silicates, it is perhaps not surprising that naturally weathered silicate minerals dissolve with different relative contributions to dissolution from different kinds of surface (e.g. dislocation-influenced *versus* bulk surface). The preponderance of morphological evidence from naturally dissolved olivines (Velbel 2009) suggests that enlargement of etch-pits by preferential dissolution of etch-pits walls is dominant relative to solutional lowering of surface between etch-pits. The inferred dominance of solutional loss from etch-pit walls is embodied in the analysis that follows below.

Velbel et al. (2007) calculated timescales of etch-pit formation on naturally weathered garnet grains, using experimentally determined garnet dissolution rates to estimate the time required to form etch-pits of observed dimensions. For simplicity, as a first approximation, hemispherical etch-pit geometry is assumed (Velbel et al. 2007). This approach assumes that all dissolution occurs at the walls of etch-pits; in other words, that all reactive surface area on naturally corroded olivines is within etch-pits, and that the olivine surface between etch-pits is not reactive. Velbel et al. (2007) discuss some inferences about the distribution of dissolution on naturally weathered silicate minerals from their studies of garnet naturally altered by aqueous solutions at near-Earth-surface ambient conditions. At advanced stages of such natural garnet dissolution, the entire grain surface consists of facets on imbricate wedge marks (IWMs; Salvino and Velbel 1989). These facets are the walls of coalesced euhedral etch-pits of dodecahedral geometry appropriate to garnet's crystallography (Pabst 1943; Velbel 1984, 1993a; Cherepanova et al. 1992; Boutz and Woensdregt 1993; Iishi and Utsumi 2006; Velbel et al. 2007). Consequently, from IWM development onward, the entire garnet surface consists of etch-pit walls, and there is no other surface (Velbel et al. 2007; similar dominance of corroded mineral surfaces by etch-pit walls beyond the initial stage of dissolution was inferred from experimental dissolution of quartz by Gautier et al., 2001). Unetched surface between etch-pits occurs at less advanced stages of garnet dissolution (Velbel 1984; Velbel et al. 2007). However, the fact that such surface does not survive at more advanced stages of garnet dissolution suggests that etch-pit edges are consumed faster by lateral growth of etch-pits (dissolution of etch-pit walls and edges) than by bulk-surface lowering (Velbel et al. 2007).

Enlargement of etch-pits by preferential dissolution of etch-pits walls is dominant relative to solutional lowering of surface between etch-pits on garnet, demonstrating that this etching mode operates on at least some silicate minerals (Velbel et al. 2007). This contrasts with the case of feldspar dissolution, during which mass is removed both from etch-pits and by retreat (lowering) of the surface between them (Lüttge et al. 1999;

Lasaga and Lüttge 2001). However, because of diversity of crystal structures, crystal chemistry, and dislocation distributions and characteristics of different silicate minerals, the relative contributions to dissolution from different kinds of surface (e.g. dislocation-influenced *versus* bulk surface) may vary among silicate minerals (Velbel et al. 2007). Olivine resembles garnet in that entire surfaces of extensively corroded olivine consist of etch-pit walls, and there is no other surface (Fig. 1 outlined area; see Velbel 2009 for other examples). The inferred dominance of solutional loss from etch-pit walls is embodied in the equations used here.

The volume [V] of a hemispherical etch-pit of radius r is

$$V = 2/3\pi r^3 \quad (1)$$

The internal surface area [A] of a hemispherical etch-pit of radius r is

$$A = 2\pi r^2 \quad (2)$$

Surface-area and volume relationships for other etch-pit geometries exhibit similarly small deviations from those of a sphere. The Appendix estimates surface area from previously published shape models of the observed conical (Fig. 1, arrows) and biconical etch-pits on naturally weathered olivine (Velbel 2009; Nowicki and Velbel 2011). An olivine etch-pit of radius r with the observed average geometry of natural olivine etch-pits has only 15% more surface area than a hemispheric etch-pit of the same radius. Etch-pits on artificially or experimentally etched olivines have a variety of different geometries and different surface-area and volume relationships, but do not deviate from equancy much more than do observed etch-pits on naturally weathered olivine. Other sources of uncertainty in mass-time relationships of silicate-mineral dissolution during weathering can be up to four orders-of-magnitude (see below; Pačes 1983; Velbel 1993b; White and Brantley 2003). In this context, the effects of differing geometric assumptions about the shapes and surface areas of the etch-pits are negligible for this application.

The number of moles of mineral removed when a volume V of mineral is dissolved is

$$M = V/V^\circ \tag{3}$$

where V° is the molar volume (cm^3/mol) of the specific mineral being dissolved. The time required to dissolve a mass M is

$$t_d = M/JA \tag{4}$$

where J is the dissolution rate ($mol/cm^2/s$). In general, the dissolution rate J can be determined from laboratory experiments or from geochemical mass-balance in natural systems where watershed-scale solute-flux data are available.

Substituting and noting that diameter d equals $2r$ gives

$$t_d = ((2/3\pi r^3)/\ V^\circ)/(J\ 2\pi r^2) \tag{5}$$

$$t_d = r\ /(3\ V^\circ\ J) = (d/2)/(3\ V^\circ\ J) = d\ /(6\ V^\circ\ J)$$

(6)

$$t_d = r/(3\ V°\ J) = d/(6\ V°\ J)$$

(7)

The time required to form etch-pits of a defined geometry and measured characteristic dimension during a dissolution experiment can be determined if the dissolution rate of the mineral is known from experimentally determined dissolution rates. Using the range of experimentally determined forsterite dissolution rates reviewed and compiled by Olsen and Rimstidt (2007) and Rimstidt et al. (2012) and invoking the geometric assumptions about olivine volume and surface area in the samples examined allows determination of the time required to form an hemispherical etch-pit of radius *r* or diameter *d*, using equation (7)

$$t_d = r/(3\ V°\ J) = d/(6\ V°\ J)$$

where *V*° is the molar volume (cm^3/mol) and *J* is dissolution rate ($mol/cm^2/s$).

Etch-pits on dissolved Fo_{91} olivine after an experiment at pH 2 were imaged by SEM and reported as Figure 3b of Pokrovsky and Schott (2000). A characteristic length dimension of 1-2 μm was determined visually for the largest imaged (roughly equant) etch-pits shown there. As with other experiments reported by Pokrovsky and Schott (2000), the pH 2 experimental run, #27, was run at room temperature (25.0 ± 0.5°C). The temperature and pH of the longest experimental run (28 hours) were used to determine the forsterite dissolution rate using equation (5) of Rimstidt et al. (2012). The rate determined in this way was used along with the molar volume of forsterite ($V°_{forsterite}$= 43.603 cm^3/mol; Smyth and Bish 1988) and the length (diameter) dimension determined from the image to solve equation (7) for the time required to form an etch-pit of the observed size under the known experimental conditions. The etch-pit formation time estimated by solving equation (7) was then compared with the 28 hr reported duration of experimental run #27 (Pokrovsky and Schott 2000).

RESULTS

Formation of olivine etch-pits of the 1-2 μm size produced during the dissolution experiments of Pokrovsky and Schott (2000) at the known pH and temperature would require ~18-35 hours according to equation (7) above.

DISCUSSION

The pH 2 experimental run of Pokrovsky and Schott (2000) lasted 28 hours; the estimated formation times for etch-pits of the observed size range from 63-126% of the observed experimental duration. Thus, within errors of estimation, the etch-pit formation time estimated from equation (7) and the selected parameters is indistinguishable from time available in the actual experiment.

Equation (7) apportions dissolution to only the internal surface of the etch-pit, assuming no influence on etch-pit size by modification of etch-pit margins through concurrent retreat of the bulk surface or any other process other than radial enlargement of the etch-pit. The olivine dissolution rate used to estimate etch-pit formation time, 6×10^{-12} mol/cm^2/s, was determined from the compilation and regressions of Rimstidt et al. (2012). Use of this rate and the imaged etch-pit sizes from Pokrovsky and Schott (2000) in equation (7) recovers the duration of the experiment that produced the imaged etch-pits to within less than a factor of two.

Apportioning Mg and Si release fluxes to the entire measured surface area of their experimentally dissolved olivine, Pokrovsky and Schott (2000) determined an experimental olivine dissolution rate 2.07(±0.17) × 10^{-12} mol/cm^2/s from experiment #27. Using this rate in equation (7) yields etch-pit formation times two to four times longer than the actual duration of experiment #27. If the bulk surface and the etch-pit interior surface were dissolving at the same surface-area-averaged rate determined experimentally during experiment #27, etch-pits of the observed size could not form during the observed experimental time-scale. The fact that the observed etch-pits were formed during the experiment requires that dissolution of etch-pit walls must be several times faster than the dissolution rate averaged over the entire grain surface, and many times faster (per unit surface area) than dissolution of the bulk surface between the etch-pits. This is consistent in a simple manner with the suggestion of Fischer et al. (2012) that a bulk, surface-area normalized dissolution rate includes contributions from surfaces of different reactivity that would be better treated as parts of a distribution (illustrated in this simple example as different proportions of two types of surfaces) rather than being lumped into a single uniform area-averaged value. This also quantitatively supports the dominance of etch-pit walls inferred from dissolution kinetics experiments on quartz (Gautier et al., 2001) and observations of moderately and extensively corroded natural garnets by Velbel et al. (2007), and suggests that similar observations of moderately and extensively etched olivine (Fig. 1 arrows and outlined area, respectively) imply a similar dominance of the etch-pit walls over the bulk surface between the etch-pits during olivine corrosion.

IMPLICATIONS FOR ESTIMATES OF OLIVINE LIFETIME AT MARS' SURFACE

Wherever olivine persists at the surface of Mars (e.g., Hoefen et al. 2003; Christensen et al. 2003, 2004a,b; Morris et al. 2004, 2006; McSween et al. 2004, 2010; Mustard et al. 2008; Koeppen and Hamilton 2008; Ehlmann et al. 2011) water was present in too minor an abundance and for too short a time to consume the primary minerals and/or leach away their soluble products (Ming et al. 2008; McLennan and Grotzinger 2008). A variety of approaches have been used to estimate more specifically when and how long liquid water was present at the surface of Mars. In one recent effort, soil samples acquired from trenches on the periglacial landforms surrounding the Phoenix Mars Lander (2008) were imaged by the optical microscope (OM) in its Microscopy, Electrochemistry, and Microscopy Analyzer (MECA) (Hecht et al. 2008), returning hundreds of color images of grains finer than 200 µm and as fine as 4 µm in size (Smith et al. 2009; Goetz et al. 2010). The upper limiting size was determined by the sieve through which sample was introduced by the Phoenix Robotic Arm (RA) into the MECA instrument; the lower limiting size was determined by the 4 µm / pixel limit of the optical system (Hecht et al. 2008). The MECA atomic force microscope (AFM; Staufer et al. 2000) returned three-dimensional images of particles as small as 0.1 µm, some of which exhibited angular morphologies consistent with aqueous corrosion of pyroxene, but in the absence of instruments on Phoenix that could identify minerals, other explanations not involving pyroxene weathering cannot be ruled out (Velbel and Losiak 2010). The paucity of clay-size particles in the size distribution of particles measured from the OM and AFM images and spanning more than three orders of magnitude, from clay-size to fine sand, implies a history of physical erosion with only minor production of fines by chemical weathering, limiting the duration of reactions of Phoenix samples with liquid water to much less than 5,000 years over the history of the soil (Pike et al. 2011).

Stopar et al. (2006) estimated the maximum duration of aqueous alteration of Mars' surface materials of a given particle size by adjusting experimentally determined olivine dissolution rates for known differences between laboratory and field rates (e.g., Pačes 1983; Velbel 1993b; White and Brantley 2003). Most room-temperature dissolution kinetics experiments are undertaken using dilute solutions at standard temperature and pressure (STP). This yields maximum limiting rates that result in minimum lifetimes of specified mineral volumes (whole sand- or silt-size grains in the applications of Stopar et al. 2006, and Olsen and Rimstidt 2007; etch-pits in the present case). The present paper demonstrates that this approach recovers the timescales of experimental etch-pit production on olivine at STP and extreme undersaturation of the solution with respect to olivine in experiments where pH is known. For application of this approach to natural weathering at conditions other than STP and extreme solution undersaturation with respect to the dissolving mineral, experimentally determined maximum rates must be adjusted. Specific required adjustments are discussed in the next paragraphs, along with summaries of how well current understanding supports such applications.

Weathering on Mars may have taken place over a wide range of possible temperatures (Carr 2006), most of which are different from than those at which mineral dissolution rates are experimentally determined in the laboratory, and reaction rates between silicate minerals and aqueous solutions vary with temperature in a manner described by the Arrhenius equation (e.g., Arrhenius 1889; Glasstone et al. 1941; Velbel

1990, 1993c). Arrhenius activation energies for the dissolution of forsteritic olivine are not well understood (Rimstidt et al. 2012).

Olivine compositions on Mars as determined from orbital spectroscopy and Mars meteorites (Hoefen et al. 2003; Christensen et al. 2004a,b; Morris et al. 2004, 2006; Treiman 2005; Koeppen and Hamilton 2008) are more fayalitic than the Fo_{91-100} for which abundant experimental low-temperature dissolution-rate data are available (Rimstidt et al. 2012). Under similar experimental conditions, fayalitic olivine may dissolve from six times (Wogelius and Walther 1992) to up to two orders-of-magnitude (Westrich et al. 1993) faster than forsteritic olivine. Similar ranges are observed among fayalite dissolution kinetics experiments when more recent studies using different sample preparation and experimental procedures are included (e.g., Daval et al., 2010). As a broader diversity of experimental procedures and conditions among individual forsterite and fayalite dissolution experiments is considered, the influences of a variety of factors including sample pretreatment and different approaches to estimating surface area remain to be resolved (Velbel, 1999; Daval et al., 2010). Insufficient experimental data exist on dissolution kinetics of ferroan olivine of intermediate composition to establish whether the dependence of dissolution rate on Fo content is linear over the compositional range.

Kinetic rate laws require mineral-solution reaction rates to slow as thermodynamic equilibrium is approached (e.g., Sposito 1994). For experimental systems in which a single mineral supplies the entire inventory of all relevant solute, this effect will tend to make weathering in chemically evolved low-temperature aqueous solution slower, and estimated time-scales of mineral persistence and mineral-grain-surface modification longer, than the rates measured at extreme undersaturation with respect to olivine in room-temperature laboratory experiments at infinite dilution. Reactions involving other minerals can effect abundances of one or more solutes and thereby influence the degree of undersaturation of the solution with respect to the dissolving mineral. For example, if Mg-carbonates or silica precipitate quickly and consume dissolved Mg or Si (respectively) then the solution might remain undersaturated with respect to dissolving forsteritic olivine and far-from-(olivine-solution)-equilibrium dissolution might be maintained. On the other hand, if equilibrium precipitation of Mg-carbonate or silica maintains high (solubility equilibrium) concentrations of Mg or Si then the presence of the secondary minerals may maintain closer-to-(olivine-solution)-equilibrium dissolution rates. In any case, the dissolution rate of olivine will be described by the olivine dissolution rate law. The specific dependence of olivine dissolution rate as a function of undersaturation remains to be established.

Comparisons of abundant published silicate-mineral weathering rates determined experimentally with those determined from weathering in natural systems reveals a systematic lab/field rate discrepancy; field rates are commonly up to three (and in a few instances, up to four) orders of magnitude slower than experimentally determined rates (Pačes 1983; Velbel 1993b; White and Brantley 2003). Most of the aforementioned factors, as well as hydrodynamics, the distinction between reactive, geometric, and total surface area, and other not-yet-defined other processes responsible for the lab/field rate discrepancy, are taken into account graphically by Olsen and Rimstidt (2007) in their Figure 2, and experimentally determined olivine dissolution rates are quantitatively adjusted for many of these sources of variation by Stopar et al. (2006).

The present paper shows that experimental olivine dissolution rates upon which the aforementioned applications rest yield observed experimental dissolution times for observed volumes of olivine when selected for the appropriate pH and temperature. If specific images with measurable etch-pit dimensions could be matched with specific experimental runs and their pH and T conditions, data from other recent experimental dissolution-kinetics experiments on olivines (Awad et al. 2000; Santelli et al. 2001; Welch and Banfield 2002) could be use as additional tests of this approach to mineral-lifetime estimates over a greater range of temperatures and Mars-relevant olivine compositions. Future applications of the approach of Stopar et al. (2006), Olsen and Rimstidt (2007) and this paper to estimating mineral-lifetimes on Mars and alteration time-scales of olivine corrosion in Mars meteorites can use existing experimental dissolution rate coefficients with confidence. Further progress is required in understanding of Arrhenius activation energies, the undersaturation (free-energy) dependence of the dissolution rate laws for Mars-relevant rock-forming minerals, and other terms related to saturated and unsaturated fluid flow through the media within which the dissolution reactions proceed. Continued improvements in understanding the fundamentals of olivine dissolution kinetics will narrow the ranges of uncertainty in mineral-lifetime estimates at Mars' surface in support of constraining the compositions and duration of potentially habitable aqueous solutions on Mars.

ACKNOWLEDGMENTS

The author thanks J. Barry Maynard for an inspiring remark encouraging perseverance in long-term scholarly enterprises; Roland Hellmann for thought-provoking conversations at the GES-6 meeting; Alan Pooley (Yale Peabody Museum) for assistance with the scanning electron microscopy; Andrew S. Madden and Jennifer T. McGuire for insightful contributions to earlier versions of this work; and Daniel R. Snyder, Aric M. Velbel, Karl Cronberger, and Anna Nowicki for helpful discussions and assistance with the olivine etch-pit shape model. This research was supported by NASA Grant NAG 9-1211 (M.A. Velbel, P.I.), NASA Mars Fundamental Research Program grant NNG05GL77G (M.A. Velbel, P.I.), and a Smithsonian Senior Fellowship. This paper was written during the author's tenure as a Smithsonian Senior Fellow at the Division of Meteorites, Department of Mineral Sciences, National Museum of Natural History, Smithsonian Institution. I am most grateful to Cari Corrigan and Ed Vicenzi for hosting my visit.

REFERENCES CITED

Arrhenius, S. (1889) Über die Reaktionsgeschwindigkeit bei der Inversion von Rohrzucker durch Säuren. Zeitschrift für Physikalische Chemie, 4, 226-248.

Awad, A., Koster van Groos, A.F., and Guggenheim, S. (2000) Forsteritic olivine: Effect of crystallographic direction on dissolution kinetics. Geochimica et Cosmochimica Acta, 64, 1765-1772.

Banfield J.F., Veblen D.R., and Jones, B.F. (1990) Transmission electron microscopy of subsolidus oxidation and weathering of olivine. Contributions to Mineralogy and Petrology, 106, 110–123.

Bearat, H., McKelvy, M.J., Chizmeshya, A.V.G., Gormley, D., Nunez, R., Carpenter, R.W., Squires, K., and Wolf, G.H. (2006) Carbon sequestration via aqueous olivine mineral carbonation: Role of passivating layer formation. Environmental Science and Technology, 40, 4802-4808.

Berner, E.K., and Berner, R.A. (2012) Global Environment: Water, Air, and Geochemical Cycles (2nd ed.), Princeton University Press, 444 p.

Berner, R.A. (1978) Rate control of mineral dissolution under earth surface conditions. American Journal of Science, 278, 1235-1252.

Boudier, F., Baronnet, A., and Mainprice, D. (2010) Serpentine mineral replacements of natural olivine and their seismic implications: Oceanic lizardite versus subduction-related antigorite. Journal of Petrology, 51, 495–512.

Boutz, M.M.R., Woensdregt, C.F. (1993) Theoretical growth forms of natural garnets. Journal of Crystal Growth, 134, 325–336.

Brantley, S.L., Kubicki, J.D., and White, A.F. (eds.) (2008) Kinetics of Mineral-Water Interactions. Springer-Verlag, 833 pp.

Brantley, S.L., Crane, S.R., Crerar, D.A., Hellmann, R., and Stallard, R. (1986) Dissolution at dislocation etch-pits in quartz. Geochimica et Cosmochimica Acta, 50, 2349-2361.

Carr M. (2006) The Surface of Mars. Cambridge University Press, 307 pp.

Cherepanova, T.A., Bennema, P., Yanson, Y.A., Vogels, L.J.P. (1992) Morphology of synthetic and natural garnets: theory and observations. Journal of Crystal Growth, 121, 17–32.

Christensen, P.R., Bandfield, J.L., Bell, J.F., III, Gorelick, N., Hamilton, V.E., Ivanov, A., Jakosky, B.M., Kieffer, H.H., Lane, M.D., Malin, M.C., McConnochie, T., McEwen, A.S., McSween, H.Y., Jr., Mehall, G.L., Moersch, J.E., Nealson, K.H., Rice, J.W., Jr., Richardson, M.I., Ruff, S.W., Smith, M.D., Titue, T.N., and Wyatt, M.B. (2003) Morphology and composition of the surface of Mars: Mars Odyssey THEMIS results. Science, 300, 2056-2061.

Christensen, P.R., Ruff, S.W., Fergason, R.L., Knudson, A.T., Anwar, S., Arvidson, R.E., Bandfield, J.L., Blaney, D.L., Budney, C., Calvin, W.M., Glotch, T.D., Golombek, M.P., Gorelick, N., Graff, T.G., Hamilton, V.E., Hayes, A., Johnson, J.R., McSween, H.Y., Jr., Mehall, G.L., Mehall, L.K., Moersch, J.E., Morris, R.V., Rogers, A.D., Smith, M.D., Squyres, S.W., Wolff, M.J., and Wyatt, M.B., 2004a. Initial results from the Mini-TES experiment in Gusev Crater from the Spirit Rover. Science, 305, 837-842.

This is a preprint, the final version is subject to change, of the American Mineralogist (MSA)
Cite as Authors (Year) Title. American Mineralogist, in press.
(DOI will not work until issue is live.) DOI: http://dx.doi.org/10.2138/am-2014-4654

Christensen, P.R., Wyatt, M.B., Glotch, T.D., Rogers, A.D., Anwar, S., Arvidson, R.E., Bandfield, J.L., Blaney, D.L., Budney, C., Calvin, W.M., Fallacaro, A., Fergason, R.L., Gorelick, N., Graff, T.G., Hamilton, V.E., Hayes, A., Johnson, J.R., Knudson, A.T., McSween, H.Y. Jr., Mehall, G.L., Mehall, L.K., Moersch, J.E., Morris, R.V., Smith, M.D., Squyres, S.W., Ruff, S.W., and Wolff, M.J., 2004b. Mineralogy at Meridiani Planum from the Mini-TES experiment on the Opportunity Rover. Science, 306, 1733-1739.

Daval, D., Testemale, D., Recham, N., Tarascon, J.-M., Martinez, I., and Guyot, F. (2010) Fayalite (Fe2SiO4) dissolution kinetics determined by X-ray absorption spectroscopy. Chemical Gelogy, 275, 161-175.

Daval, D., Sissman, O., Menguy, N., Saldi, G.D., Guyot, F., Martinez, I., Corvisier, J., Garcia, B., Machouk, I., Knauss, K.G., and Hellmann, R. (2011) Influence of amorphous silica layer formation on the dissolution rate of olivine at 90°C and elevated pCO_2. Chemical Geology, 284, 193-209.

Deer, W.A., Howie, R.A., and Zussman, J. (1992) An Introduction to the Rock-Forming Minerals, 2nd edition: Longman Scientific & Technical, 696 pp.

Delvigne, J., Bisdom, E.B.A., Sleeman, J., and Stoops, G., (1979) Olivines: Their pseudomorphs and secondary products. Pedologie, 39, 247-309.

Eggleton, R.A. (1986) The relation between crystal structure and silicate weathering rates. In Rates of Chemical Weathering of Rocks and Minerals, edited by Colman S. M. and Dethier D. P. Orlando, Florida: Academic Press. pp. 21-40.

Ehlmann, B.L., Mustard, J.F., Clark, R.N., Swayze, G.A., and Murchie, S.L. (2011) Evidence for low-grade metamorphism, hydrothermal alteration, and diagenesis on Mars from phyllosilicate assemblages. Clays and Clay Minerals, 59, 359-377.

Fischer, C., Arvidson, R.S., and Lüttge, A. (2012) How predictable are dissolution rates of crystalline material? Geochimica et Cosmochimica Acta, 98, 177-185.

Gautier, J.-M., Oelkers,E.H., and Schott, J. (2001) Are quartz dissolution rates proportional to B.E.T. surface areas? Geochimica et Cosmochimica Acta, 65, 1059-1070.

Giammar, D.E., Bruant, R.G., Jr., and Peters, C.A. (2005) Forsterite dissolution and magnesite precipitation at conditions relevant for deep saline aquifer storage and sequestration of carbon dioxide. Chemical Geology, 217, 257-276.

Glasstone, S., Laidler, K.J., and Eyring, H. (1941) The Theory of Rate Processes. McGraw-Hll Book Company, New York, 611 pp.

Goetz, W., Pike, W.T., Hviid, S.F., Madsen, M.B., Morris, R.V., Hecht, M.H., Staufer, U., Leer, K., Sykulska, H., Hemmig, E., Marshall, J., Morookian, J.M., Parrat, D., Vijendran, S., Bos, B.J., El Maarry, M.R., Keller, H.U., Kramm, R., Markiewicz, W.J., Drube, L., Blaney, D., Arvidson, R.E., Bell, J.F., III, Reynolds, R., Smith, P.H., Woida, P., Woida, R., and Tanner, R. (2010) Microscopic structure of soils at the Phoenix landing site, Mars: classification and description of their optical and magnetic properties. Journal of Geophysical Research, 113, E00E22. doi:10.1029/2009je003437.

Goldich, S.S., (1938) A study in rock weathering. Journal of Geology, 46, 17-58.

Grossman, J.J., Ryan, J.A., Mukherjee, N.R., and Wegner, M.W. (1971) Microchemical, microphysical, and adhesive properties of lunar material. Proceedings of the Second Lunar Science Conference, 3, 2153-2164.

Haug, T.A., Kleiv, R.A., and Munz, I.A. (2010) Investigating dissolution of mechanically activated olivine for carbonation purposes. Applied Geochemistry, 25, 1547-1563.

Hecht, M.H., Marshall, J., Pike, W.T., Staufer, U., Blaney, D., Braendlin, D., Gautsch, S., Goetz, W., Hidber, H.-R., Keller, H.U., Markiewicz, W.J., Mazer, A., Meloy, T.P., Morookian, J.M., Mogensen, C., Parrat, D., Smith, P., Sykulska, H., Tanner, R.J., Reynolds, R.O., Tonin, A., Vijendran, S., Weilert, M., and Woida, P.M. (2008) Microscopy capabilities of the Microscopy, Electrochemistry, and Conductivity Analyzer. Journal of Geophysical Research – Planets, 113, E00A22, doi:10.1029/2008JE003077.

Hoefen, T.M., Clark, R.N., Bandfield, J.L., Smith, M.D., Pearl, J.C., and Christensen, P. R., 2003. Discovery of olivine in the Nili Fossae region of Mars. Science, 302, 627-630.

Hutchison, R. (2004) Meteorites: A Petrologic, Chemical and Isotopic Synthesis: Cambridge University Press, Cambridge, U.K., 506 pp.

Iishi, K., and Utsumi, J. (2006) Morphology of flux-grown vanadate garnets. Journal of Crystal Growth, 291, 436-441.

Inoue, T., Komatsu, H., Hosoya, S. and Takei, H. (1981) Defect structures of synthetic olivine. Journal of Crystal Growth, 55, 307-316.

King, H.E., Plümper, O., and Putnis, A. (2010) Effect of secondary phase formation on the carbonation of olivine. Environmental Science and Technology, 44, 6503-6509.

King, H.E., Plümper, O., Geislere, T., and Putnis, A. (2011) Experimental investigations into the silicification of olivine: Implications for the reaction mechanism and acid neutralization. American Mineralogist, 96, 1503-1511.

Kirby, S.H. and Wegner, M.W. (1978) Dislocation substructure of mantle-derived olivine as revealed by selective chemical etching and transmission electron microscopy. Physics and Chemistry of Minerals, 3, 309-330.

Koeppen, W.C. and Hamilton, V.E. (2008) Global distribution, composition, and abundance of olivine on the surface of Mars from thermal infrared data. Journal of Geophysical Research, 113, E05001, 2007JE002984.

Lafay, R., Montes-Hernandez, G., Janots, E., Chiriaz, R., Findling, N., and Toche, F. (2012) Mineral replacement rate of olivine by chrysotile and brucite under high alkaline conditions. Journal of Crystal Growth, 347, 62-72.

Lasaga, A.C. and Lüttge, A., 2001. Variation of crystal dissolution rate based on a dissolution stepwave model. Science, 291, 2400-2404.

Lee, M.R., Tomkinson, T., Mark, D.F., Stuart, F.M., and Smith, C.L. (2013) Evidence for silicate dissolution on Mars from the Nakhla meteorite. Meteoritics and Planetary Science, 48, 224-240.

Lüttge, A., Bolton, E.W., and Lasaga, A.C. (1999) An interferometric study of the dissolution kinetics of anorthite: the role of reactive surface area. American Journal of Science, 299, 652-678.

McLennan, S.M., and Grotzinger, J.P. (2008) The sedimentary rock cycle of Mars, in Bell, J.F., III, ed., The Martian Surface: Composition, Mineralogy, and Physical Processes: Cambridge, U.K., Cambridge University Press, p. 541-577.

McSween, H.Y., Jr., Arvidson, R.E., Bell, J.F., III, Blaney, D., Cabrol, N.A., Christensen, P.R., Clark, B.C., Crisp, J.A., Crumpler, L.S., Des Marais, D.J., Farmer, J.D., Gellert, R., Ghosh, A., Gorevan, S., Graff, T., Grant, J., Haskin, L.A., Herkenhoff, K.E., Johnson, J.R., Jolliff, B.L., Klingelhoefer, G., Knudson, A.T., McLennan, S., Milam, K.A., Moersch, J.E., Morris, R.V., Rieder, R.,. Ruff, S.W., de Souza, P.A. Jr., Squyres, S.W., Wänke, H., Wang, A., Wyatt, M.B., and Zipfel, J. (2004) Basaltic rocks analyzed by the Spirit rover in Gusev Crater. Science, 305, 842-845.

McSween, H.Y., Jr., McGlynn, I.O., and Rogers, A.D. (2010) Determining the modal mineralogy of Martian soils. Journal of Geophysical Research, 115, E00F12, 2010JE003582.

Ming, D.W., Morris, R.V., and Clark, B.C. (2008) Aqueous alteration on Mars, in Bell, J.F., III, ed., The Martian Surface: Composition, Mineralogy, and Physical Processes: Cambridge, U.K., Cambridge University Press, p. 519-540.

Morris, R.V., Klingelhöfer, G., Bernhardt, B., Schröder, C., Rosionov, D.S., de Souza, P. A. Jr., Yen, A., Gellert, R., Evlanov, E.N., Foh, J., Kankeleit, E., Gütlich, P., Ming, D.W., Renz, F., Wdowiak, T., Squyres, S.W., and Arvidson, R.E. (2004) Mineralogy at Gusev Crater from the Mössbauer spectrometer on the Spirit Rover. Science, 305, 833-836.

Morris, R.V., Klingelhöfer, G., Schröder, C., Rodionov, D.S., Yen, A., Ming, D.W., de Souza, P.A., Jr., Fleischer, I., Wdowiak, T., Gellert, R., Bernhardt, B., Evlanov, E.N., Zubkov, B., Foh, J., Bonnes, U., Kankeleit, E., Gütlich, P., Renz, F., Squyres, S.W., and Arvidson, R.E. (2006) Mössbauer mineralogy of rock, soil, and dust at Gusev crater, Mars: Spirit's journey through weakly altered olivine basalt on the plains and pervasively altered basalt in the Columbia Hills. Journal of Geophysical Research, 111, E02S13, 2005JE002584.

Morton, A.C. and Hallsworth, C.R. (1999) Processes controlling the composition of heavy minerals in sandstones. Sedimentary Geology, 124, 3-29.

Mustard, J.F., Murchie, S.L., Pelkey, S.M., Ehlmann, B.L., Milliken, R.E., Grant, J.A., Bibring, J.-P., Poulet, F., Bishop, J., Noe Dobrea, E., Roach, L., Seelos, F., Arvidson, R.E., Wiseman, S., Green, R., Hash, C., Humm, D., Malaret, E., McGovern, J.A., Seelos, K., Clancy, T., Clark, R., des Marais, D.J., Izenberg, N., Knudson, A., Langevin, Y., Martin, T., McGuire, P., Morris, R., Robinson, M., Roush, T., Smith, M., Swayze, G., Taylor, H., Titus, T., and Wolff, M., 2008. Hydrated silicate minerals on Mars observed by the Mars Reconnaissance Orbiter CRISM instrument. Nature, 454, 305-309.

Nowicki, M.A., and Velbel, M.A. (2011) Preliminary quantification of a shape model for etch-pits formed during natural weathering of olivine. Applied Geochemistry, 26, S112-S114.

Olsen, A. A. and Rimstidt, J. D. (2007) Using a mineral lifetime diagram to evaluate the persistence of olivine on Mars. American Mineralogist, 92, 598-602.

Pabst, A. (1943) Large and small garnets from Fort Wrangell, Alaska. American Mineralogist, 28, 233–245.

Pačes, T. (1983) Rate constants of dissolution derived from the measurements of mass balance in hydrological catchments. Geochimica et Cosmochimica Acta, 47, 1855-1863.

Pike, W.T., Staufer, U., Hecht, M.H., Goetz, W., Parrat, D., Sykulska-Lawrence, H., Vijendran, S., and Madsen, M.B. (2011) Quantification of the dry history of the Martian soil inferred from in situ microscopy. Geophysical Research Letters, 38, L24201.

Pokrovsky, O.P., and Schott, J. (2000) Kinetics and mechanism of forsterite dissolution at 25^{o}C and pH from 1 to 12. Geochimica et Cosmochimica Acta, 64, 3313-3325.

Rimstidt, J.D., Brantley, S.L., and Olsen, A.A. (2012) Systematic review of forsterite dissolution rate data. Geochimica et Cosmochimica Acta, 99, 159-178.

Salvino, J.F. and Velbel, M.A. (1989) Faceted garnets from sandstones of the Munising Formation (Cambrian), northern Michigan: Petrographic evidence for origin by intrastratal dissolution. Sedimentology, 36, 371-379.

Santelli, C.M., Welch, S.A., Westrich, H.R., and Banfield, J.F. (2001) The effect of Fe-oxidizing bacteria on Fe-silicate mineral dissolution. Chemical Geology, 180, 99-115.

Smith, P.H., Tamppari, L.K., Arvidson, R.E., Bass, D., Blaney, D., Boynton, W.V., Carswell, A., Catling, D.C., Clark, B.C., Duck, T., DeJong, E., Fisher, D., Goetz, W., Gunnalugsson, H.P., Hecht, M.H., Hipkin, V., Hoffman, J., Hviid, S.F., Keller, H.U., Kounaves, S.P., Lange, C.F., Lemmon, M.T., Ming, D.W., Morris, R.V., Pike, W.T., Renno, N., Staufer, U., Stoker, C., Taylor, P., Whiteway, J.A., and Zent, A.P. (2009) H_2O at the Phoenix landing site. Science, 325, 58-61.

Smyth, J.R., and Bish, D.L. (1988) Crystal Structures and Cation Sites of the Rock-Forming Minerals. Boston: Allen & Unwin. 332 pp.

Sposito, G. (1994) Chemical Equilibria and Kinetics in Soils. New York: Oxford University Press. 268 pp.

Staufer, U., Akiyama, T., Beuret, C., Gautsch, S., Noell, W., Schürmann, Stebler, C., and de Rooij, N.F. (2000) Micro-electromechanical systems for nanoscience. Journal of Nanoparticle Research, 2, 413-418.

Stopar, J.D., Taylor, G.J., Hamilton, V.E., and Browning, L. (2006) Kinetic models of olivine dissolution and extent of aqueous alteration on Mars. Geochimica et Cosmochimica Acta, 70, 6136-6153.

Tang, Q., and Dieckmann, R. (2011) Floating-zone growth and characterization of single crystals of cobalt orthosilicates, Co_2SiO_4. Journal of Crystal Growth, 317, 119-127.

Tang, Q., and Dieckmann, R. (2012) Floating-zone growth and characterization of single crystals of manganese orthosilicates, Mn_2SiO_4. Journal of Crystal Growth, 316, 89-97.

Treiman, A.H. (2005) The nakhlite meteorites: Augite-rich igneous rocks from Mars. Chemie der Erde, 65, 203-270.

Velbel, M.A. (1984) Natural weathering mechanisms of almandine garnet. Geology, 12, 631-634.

Velbel, M.A. (1990) Influence of temperature and mineral surface characteristics on feldspar weathering rates in natural and artificial systems: A first approximation. Water Resources Research, 26, 3049-3053.

Velbel, M.A. (1993a) Formation of protective surface layers during silicate-mineral weathering under well-leached, oxidizing conditions. American Mineralogist, 78, 408-417.

Velbel, M.A. (1993b) Constancy of silicate-mineral weathering-rate ratios between natural and experimental weathering: Implications for hydrologic control of differences in absolute rates. Chemical Geology, 105, 89-99.

Velbel, M.A. (1993c) Temperature dependence of silicate weathering in nature: How strong a negative feedback on long-term accumulation of atmospheric CO_2 and global greenhouse warming? Geology, 21, 1059-1062.

Velbel, M.A. (1999) Bond strength and the relative weathering rates of simple orthosilicates. American Journal of Science, 299, 679-696.

Velbel, M.A. (2009) Dissolution of olivine during natural weathering. Geochimica et Cosmochimica Acta, 73, 6098-6113.

Velbel, M.A. (2012) Aqueous alteration in Martian meteorites: Comparing mineral relations in igneous-rock weathering of Martian meteorites and in the sedimentary cycle of Mars. In Sedimentary Geology of Mars, edited by Grotzinger J., and Milliken R., SEPM – Society for Sedimentary Geology Special Publication 102, pp. 97-117.

Velbel, M.A., and Losiak, A.I. (2010) Denticles on chain silicate grain surfaces and their utility as indicators of weathering conditions on Earth and Mars. Journal of Sedimentary Research, 80, 771-780. http://DOI: 10.2110/jsr.2010.074

Velbel, M.A., and Ranck, J.M. (2008) Etch pits on naturally altered olivine from dunites of the Appalachian Blue Ridge Mountains, North Carolina, USA. Mineralogical Magazine, 72, 149-152.

Velbel, M.A., McGuire, J.T., and Madden, A.S. (2007) Scanning electron microscopy of garnet from southern Michigan soils: Etching rates and inheritance of pre-glacial and pre-pedogenic grain-surface textures. In Heavy Minerals in Use, edited by Mange M. and Wright D. Developments in Sedimentology, 58, 413-432.

Wegner, M.W., and Christie, J.M. (1974) Preferential chemical etching of terrestrial and lunar olivines. Contributions to Mineralogy and Petrology, 43, 195-212.

Wegner. M.W. and Christie, J.M. (1976) Chemical etching of dislocations in forsterite. Contributions to Mineralogy and Petrology, 59, 131-140.

Welch, S.A. and Banfield, J.F. (2002) Modification of olivine surface morphology and reactivity by microbial activity during chemical weathering. Geochimica et Cosmochimica Acta, 66, 213-221

Westrich, H.R., Cygan, R.T., Casey, W.H., Zemitis, C., and Arnold, G.W. (1993) The dissolution kinetics of mixed-cation orthosilicate minerals. American Journal of Science, 293, 869–893.

White, A.F., and Brantley, S.L. (2003) The effect of time on the weathering of silicate minerals: why do weathering rates differ in the laboratory and field? Chemical Geology, 202, 479-506.

Wilson, M.J. (1975) Chemical weathering of some primary rock-forming minerals. Soil Science, 119, 349-355.

Wilson, M.J. (2004) Weathering of the primary rock-forming minerals; processes, products and rates. Clay Minerals, 39, 233-266.

Wogelius, R.A., and Walther, J.V. (1992) Olivine dissolution kinetics at near-surface conditions. Chemical Geology, 97, 101-112.

Young, C., III (1969) Dislocations in the deformation of olivine. American Journal of Science, 267, 841-852.

This is a preprint, the final version is subject to change, of the American Mineralogist (MSA)
Cite as Authors (Year) Title. American Mineralogist, in press.
(DOI will not work until issue is live.) DOI: http://dx.doi.org/10.2138/am-2014-4654

Figures

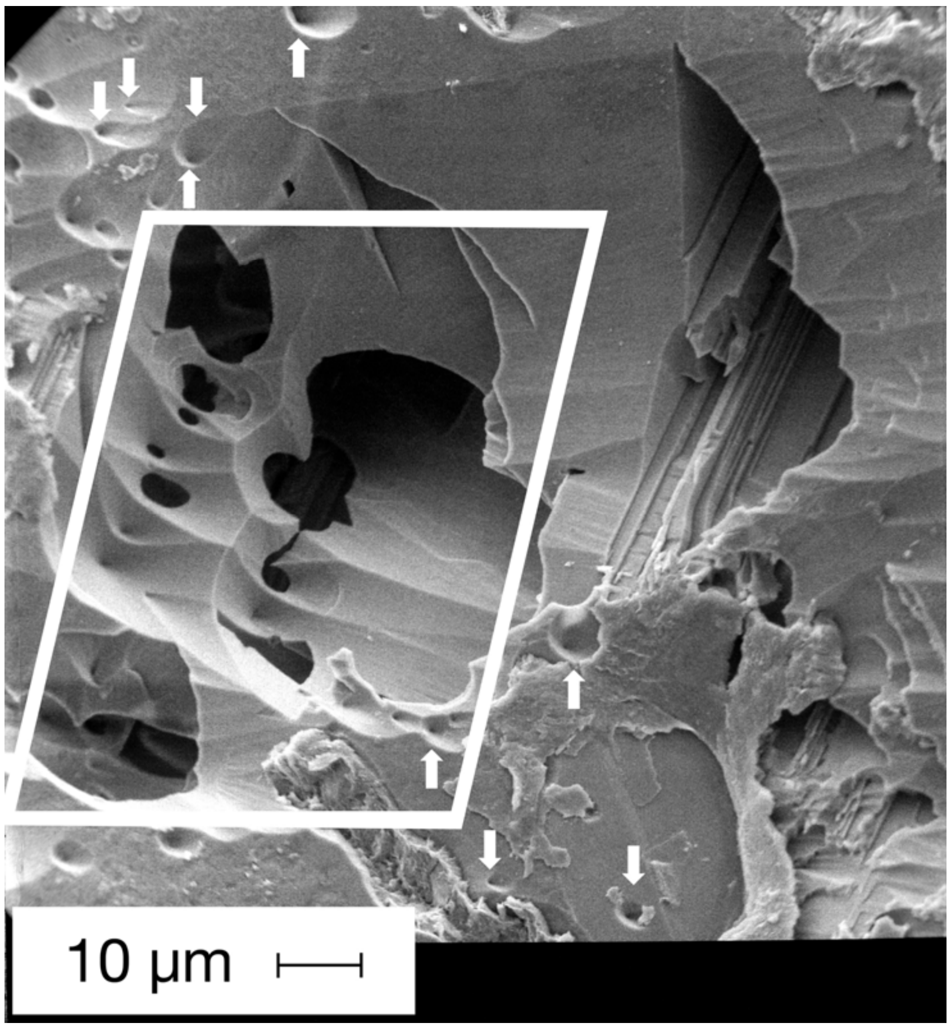

Figure 1. Dissolution-sculpted surface consisting almost entirely of conical etch-pits and their coalesced walls on naturally weathered olivine from the Day Book (North Carolina, U.S.A.) dunite. Small individual conical etch-pits occur along the bottom edge of the

image, and at upper left (arrows); sculpted surfaces consisting of intersecting etch-pit walls dominate the center and left-center of this image (outlined area). See Velbel and Ranck (2008) and Velbel (2009) for further description and other images of olivine weathering in these samples. Secondary-electron image; scale bar is 10 μm in length.

APPENDIX

The pre-etched basal area of a hemispherical etch-pit has one-half the surface area of the hemisphere described by equation (2). Even if the hemispherical etch-pit were produced by ever-smaller circular cross-sections working from the initial base inward rather than from radial retreat of the etch-pit wall, the area of surface from which mass is removed would vary by only a factor of two from equation (2).

Velbel (2009) showed that the characteristic etch-pit formed during natural low-temperature aqueous weathering of olivine is a cone (Fig. 1, arrows). Pairs of cones joined at the base are common; cross-sections through these bicones are diamond-shaped (Velbel, 2009). Two-dimensional cross-sections through these etch-pits in polished sections are often triangular wedge or notch-shaped. These cross-sections, and secondary-electron images of intact grain-surface topography suggest, that most etch-pits exposed at olivine grain surfaces are either single cones or halves of bicones (Figure 12 in Velbel, 2009). Two ideal cross-section geometries are possible. In one, the (obtuse) apex of the wedge is the apex of a single cone; in the other, the (acute) apex of the wedge is the edge along which the two cones of a (truncated half of a) bicone are joined (Figure 12 in Velbel, 2009). In either ideal case, the surface area of the etch-pit wall is one-half the surface area of a bicone.

For a circular right cone (or half of a bicone) with radius r, height h, and slant height s, the surface area of the walls is given by

$$A_{\text{cone,walls}} = A_{\text{half-bicone,walls}} = \pi rs = \pi r(r^2 + h^2)^{0.5}$$

Nowicki and Velbel (2011) empirically determined that the shapes of olivine etch-pit cross-sections vary around an average of $r{:}h = 1.78$. Substituting $r/1.78 = h$ (from $r = 1.78h$),

$$A_{\text{half-bicone,walls}} = \pi r_{\text{half-bicone}} s = \pi r_{\text{half-bicone}} (r^2_{\text{half-bicone}} + (0.562 r_{\text{half-bicone}})^2)^{0.5}$$

$$A_{\text{half-bicone,walls}} = \pi r_{\text{half-bicone}} (r^2_{\text{half-bicone}} + 0.316 r^2_{\text{half-bicone}}))^{0.5}$$

$$A_{\text{half-bicone,walls}} = \pi r_{\text{half-bicone}} (1.316 r^2_{\text{half-bicone}}))^{0.5} = \pi r_{\text{half-bicone}}\, 1.15 r_{\text{half-bicone}} = \pi 1.15 r^2_{\text{half-bicone}}$$

Given that

$$A_{\text{hemisphere}} = \pi r_{\text{hemisphere}}{}^2$$

a circular right conical or half-biconical olivine etch-pit of radius r with the observed average geometry of natural olivine etch-pits has only 15% more surface area than a hemispheric etch-pit of the same radius. Etch-pits on artificially or experimentally etched olivines exhibit a variety of different geometries and different surface-area and volume relationships, but do not deviate from equancy much more than do observed etch-pits on naturally weathered olivine.

Different assumptions about the specific geometry of an etch-pit result in surface-area estimates that vary by less than a factor of two from a simple hemispherical pit. Given that other sources of uncertainty in mass-time relationships of silicate-mineral dissolution during natural weathering can be up to four orders-of-magnitude, the effects of differing geometric assumptions about the shapes and surface areas of the etch-pits are trivial for this application. Only if other parameters are known to within much less than a factor of two will details of etch-pit shape discernably affect etch-pit formation times estimated using the approach presented here.

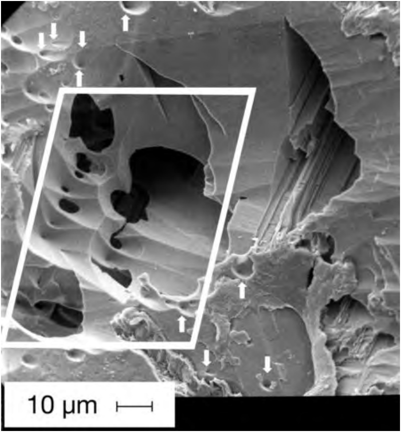
10 µm

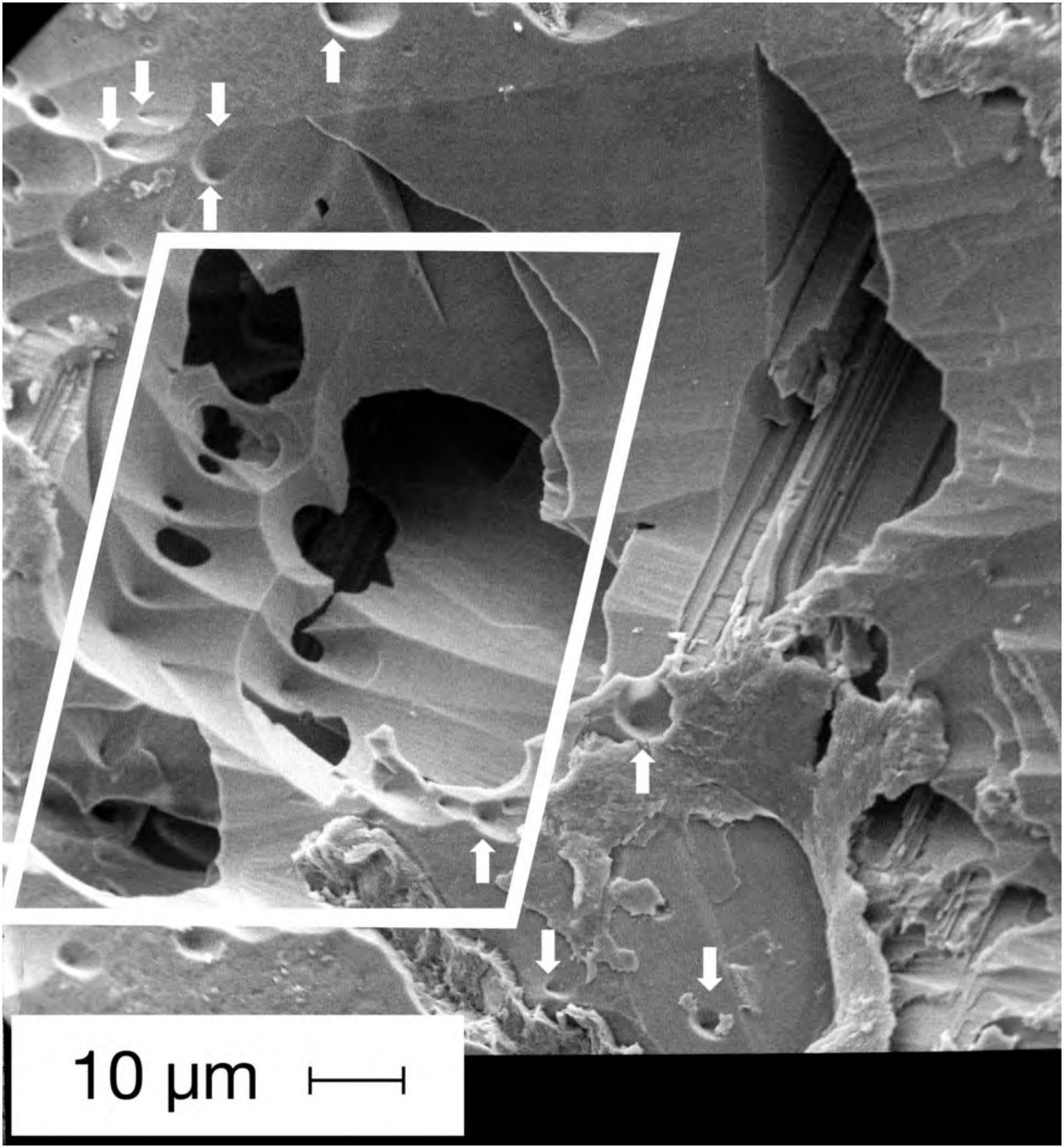
10 µm

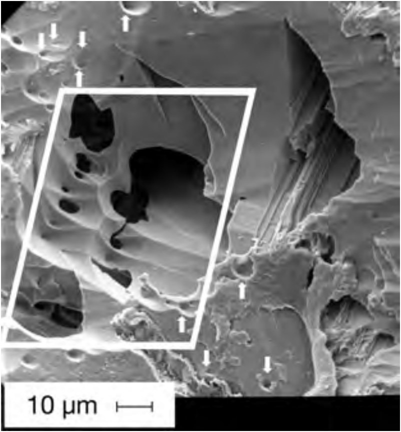
10 µm

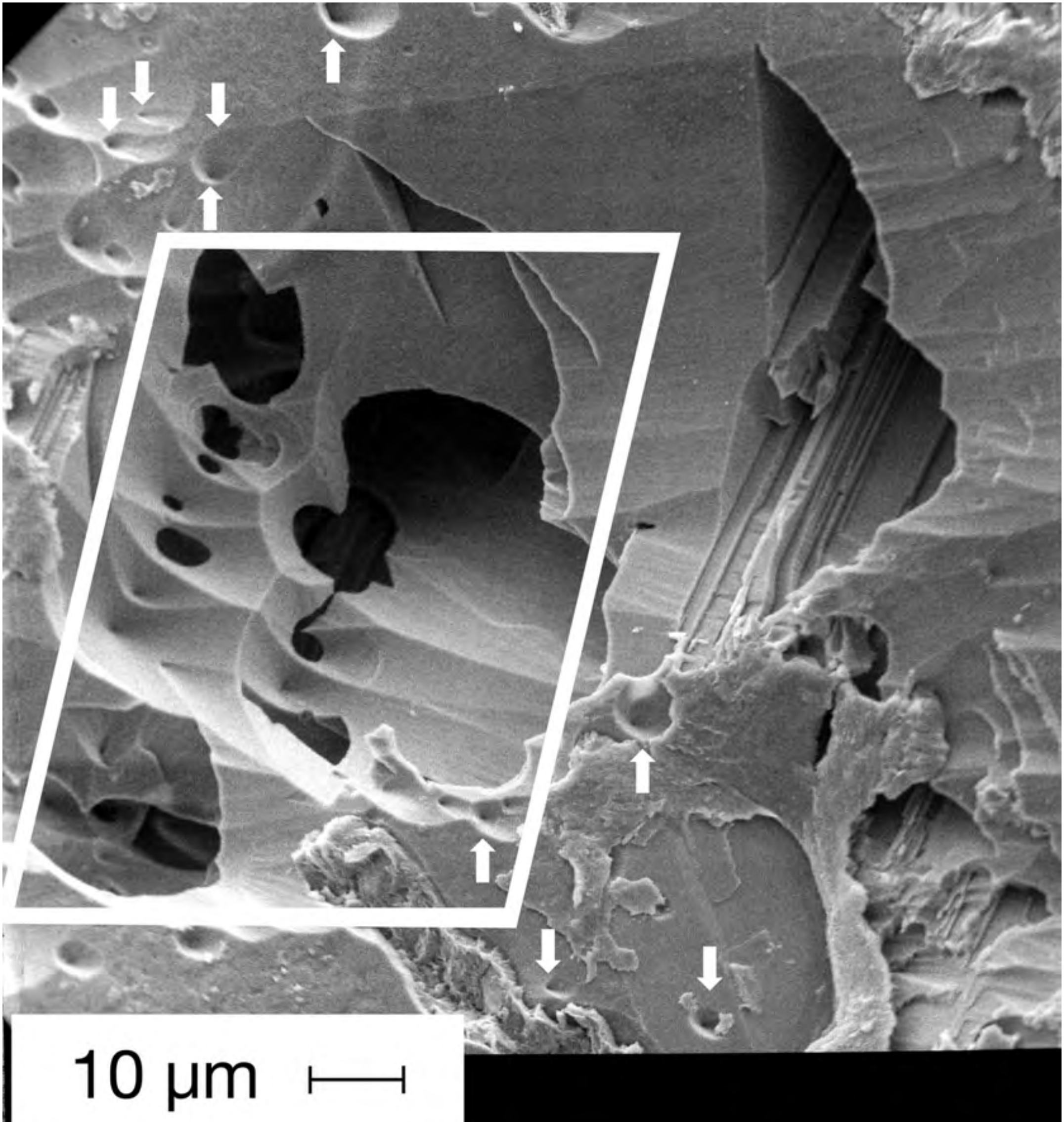
10 µm